JOURNAL OF GUIDANCE, CONTROL, AND DYNAMICS
Vol. 20, No. 6, November–December 1997

Optimal Reorientation Maneuver of Bias Momentum Spacecraft

Hyochoong Bang* and Jong-ah Kim†
Korea Aerospace Research Institute, Daejon 305-600, Republic of Korea
and
Myungsuk Kim‡
Korea Telecom, Seoul 680-63, Republic of Korea

Application of an optimal control theory is made to find the optimal rotational maneuver strategy of a pitch bias momentum spacecraft. Time-optimal and fuel/time-optimal control laws are each investigated separately. Conventional time-optimal control theory is adopted taking into account the gyroscopic effect embedded in the bias momentum spacecraft. The modal decomposition technique is not applicable to gyroscopic systems due to the skew-symmetric system matrix. Therefore, the analysis is conducted with physical coordinates with extra effort in comparison with working with modal coordinates. It turns out that the symmetric torque profile, which is a necessary condition for the rest-to-rest maneuver of generic structural systems, does not apply to gyroscopic systems.

I. Introduction

A NUMBER of theories and applications have been developed in conjunction with the time-optimal and/or fuel/time-optimal maneuver of both rigid and flexible spacecraft.[1–6] Most optimal control solutions are represented by the switching profiles of actuators, for which the actuators are usually saturated at the maximum level. The key path to finding the optimal solution is to use parameter optimization techniques instead of directly solving differential equations.[7–14] The switching times or design parameters are optimized in such a way that a given cost function is minimized while the terminal boundary conditions are satisfied.

Singh et al.[10,11] studied optimal control solutions for a flexible structure rotational maneuver. Liu and Wie[12] and Wie et al.[13] studied optimal and robust optimal switching strategies for a flexible structure model. Ben-Asher et al.[14] also applied a parameter optimization technique to a flexible structure model. They discussed a condition for the parameter optimization approach to lead to a true optimal solution. Singh and Vadali[15] used frequency-domain analysis for the optimal control solution. They developed the so-called time-delay filter to cancel both the rigid and the vibrational modes for the final pointing maneuver. The time-delay filter directly represents the optimal control profile with actuators saturated. The control torque inputs consist of combinations of different numbers of pulses in time-delayed fashions. Singh[16] also applied the time-delay filter approach to solving a benchmark problem for fuel/time-optimal control for a flexible structural model.

Most recent optimal control applications have been dominated by flexible structural systems.[9–16] They usually include both rigid-body rotational/translational motion and flexible vibratory motions.[10–16] For structural systems, the analytical modal coordinate form was exploited by the modal decomposition technique. The solutions for the rigid-body and flexible modal coordinate responses by applied external inputs were found analytically. This has the advantage of not having to solve coupled dynamic equations of the physical coordinates. Also, the applied torque inputs are symmetric about the half-maneuver time for a rest-to-rest maneuver. This results in a smaller number of design parameters, as was wisely exploited in the previous studies.[10,11,15,16]

Not much attention has been paid to applying optimal control theory to gyroscopic systems such as bias momentum spacecraft. As a sample gyroscopic system, bias momentum control is a popular method for maintaining the stability of a spacecraft. This is particularly because of the simplicity and reliability in spacecraft operation.[17] The inherent dynamic coupling created by angular momentum within the spacecraft automatically eliminates the need for sensing attitude information of one axis.[17] The control strategy for gyroscopic systems is expected to be different from that of nongyroscopic systems. One of the most significant aspects of gyroscopic systems is the induced skew-symmetric damping matrix. This results in complex conjugate eigenvalues of system matrices, which in turn make the modal decomposition in second-order form infeasible. In contrast with typical structural systems solutions, the symmetric torque profile does not satisfy the pointing requirement for gyroscopic systems.

In this study, we solve the optimal control problem for pitch bias momentum spacecraft. The analytical tool is based on the extension of the previous results of solution techniques.[15,16] In particular, the frequency-domain analysis using the time-delay filter in Refs. 15 and 16 is adopted in an effort to characterize the optimal solution for a bias momentum spacecraft. Both minimum-time and weighted fuel/time-performance indices are used to develop generic attitude maneuver strategies for rest-to-rest maneuvers. The results of the optimal maneuvers are represented by switching profiles of body-fixed actuators. The switching profiles account for control over nutational mode and rigid-body rotational maneuver.

II. Equations of Motion and Problem Statement

The simplified schematic configuration of a pitch bias momentum spacecraft is provided in Fig. 1. In this analysis, the bias momentum produced by a spinning momentum wheel exists along the orbit normal (or pitch) direction only. This creates gyroscopic coupling between the roll and yaw dynamics, i.e., so-called nutational motion.[17] The pitch bias momentum is a typical bias momentum spacecraft with three-axis, on-orbit attitude control capability.

To derive governing equations of motion, we start with the angular momentum vector of the system, defined as

$$\boldsymbol{H} = I_x\omega_x\boldsymbol{b}_1 + (I_y\omega_y + h_w)\boldsymbol{b}_2 + I_z\omega_z\boldsymbol{b}_3 \tag{1}$$

where I_x, I_y, and I_z represent body axis principal moments of inertia; ω_x, ω_y, and ω_z denote body axis components of the angular velocity vector; and h_w is the angular momentum of the wheel,

Received Nov. 11, 1996; presented as Paper 97-0109 at the AIAA 35th Aerospace Sciences Meeting, Reno, NV, Jan. 6–9, 1997; revision received March 14, 1997; accepted for publication April 10, 1997.

*Research Scientist, Koreasat Group/Space Division, P.O. Box 113, Yousung-gu. Member AIAA.
†Research Scientist, Koreasat Group/Space Division, P.O. Box 113, Yousung-gu.
‡Director, Satellite Research Group, Jayang-dong, Kwangjin-gu.

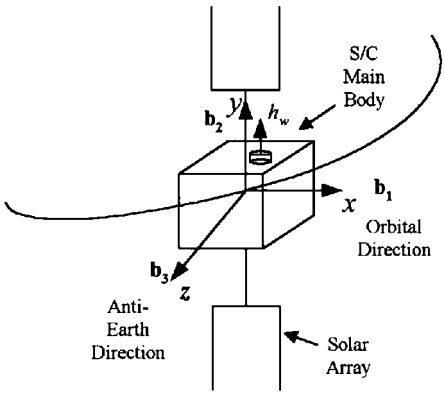

Fig. 1 Geometric configuration of a pitch bias momentum spacecraft.

which is assumed to be constant throughout. Application of Euler's equation to Eq. (1) yields

$$\frac{\mathrm{d}}{\mathrm{d}t}\boldsymbol{H} + \boldsymbol{\omega} \times \boldsymbol{H} = \boldsymbol{u} \tag{2}$$

where $\boldsymbol{\omega} = \omega_x \boldsymbol{b}_1 + \omega_y \boldsymbol{b}_2 + \omega_z \boldsymbol{b}_3$ is the angular velocity vector and $\boldsymbol{u} = [u_x, u_y, u_z]^T$ denotes the external torque input vector. The result of Eq. (2) can be written as

$$\begin{aligned} I_x\dot{\omega}_x + (I_z - I_y)\omega_y\omega_z - h_w\omega_z &= u_x \\ I_y\dot{\omega}_y + (I_x - I_z)\omega_z\omega_x + \dot{h}_w &= u_y \\ I_z\dot{\omega}_z + (I_y - I_x)\omega_x\omega_y + h_w\omega_x &= u_z \end{aligned} \tag{3}$$

The gravity gradient torque is eliminated throughout because the spacecraft model in this study is a geosynchronous spacecraft. The body axis components of angular velocities are related to the Euler angles by

$$\begin{aligned} \omega_x &= \dot{\phi} - \sin\theta\dot{\psi} + \cos\theta\sin\psi\omega_0 \\ \omega_y &= \cos\phi\dot{\theta} + \cos\theta\sin\phi\dot{\psi} + (\cos\phi\cos\psi + \sin\phi\sin\theta\sin\psi)\omega_0 \\ \omega_z &= -\sin\phi\dot{\theta} + \cos\theta\cos\phi\dot{\psi} \\ &\quad + (-\sin\phi\cos\psi + \cos\phi\sin\theta\sin\psi)\omega_0 \end{aligned} \tag{4}$$

where ω_0 denotes the angular orbital rate and the Euler angles ϕ, θ, and ψ represent roll, pitch, and yaw angles, respectively, with respect to the orbiting local vertical local horizontal frame.[17] Substitution of Eq. (4) into Eq. (3) followed by linearization by small-angle approximation yields

$$\begin{aligned} I_x\ddot{\phi} + \left[(I_y - I_z)\omega_0^2 + \omega_0 h_w\right]\phi + h_x\dot{\psi} &= u_x, \qquad I_y\ddot{\theta} + \dot{h}_w = u_y \\ I_z\ddot{\psi} + \left[(I_y - I_x)\omega_0^2 + \omega_0 h_w\right]\psi - h_z\dot{\phi} &= u_z \end{aligned} \tag{5}$$

where $h_x = h_z \equiv (I_x + I_z - I_y)\omega_0 - h_w$. As expected, the pitch dynamic equation is decoupled from the roll/yaw dynamic equations of motion. Thus, control law design for each set of dynamic equations can be conducted separately. In this study, the case is limited to the constant angular momentum of the wheel so that the pitch equation is simplified to

$$I_y\ddot{\theta} = u_y \tag{6}$$

The time-optimal control law for the rest-to-rest maneuver of the pitch dynamics is well known to be a single switching maneuver. The switching instant is at the half-maneuver time, and the control torque profile is antisymmetric about the half-maneuver time. The relationship between the final maneuver time and angular displacement is given by[18]

$$T_f = 2\sqrt{I_y\theta_f / M_y} \tag{7}$$

where θ_f is the constant final angle and M_y is the magnitude of control torque input. On the other hand, the combined fuel/time-optimal solution for a simple rigid body is a bang-off-bang profile.[18] In this case, the switching instants are determined by parameters appearing in the cost function.

Next, we discuss the roll/yaw dynamics, which are decoupled from pitch dynamics. The roll/yaw dynamics are restated from Eq. (5) as

$$I_x\ddot{\phi} + \left[(I_y - I_z)\omega_0^2 + \omega_0 h_w\right]\phi + h_x\dot{\psi} = u_x \tag{8}$$

$$I_z\ddot{\psi} + \left[(I_y - I_x)\omega_0^2 + \omega_0 h_w\right]\psi - h_z\dot{\phi} = u_z \tag{9}$$

For simplicity of analysis, Eqs. (8) and (9) are approximated as

$$I_x\ddot{\phi} + h_x\dot{\psi} = u_x \tag{10}$$

$$I_z\ddot{\psi} - h_z\dot{\phi} = u_z \tag{11}$$

The approximation is accurate enough due to the small orbital rate ω_0, which is for the geosynchronous orbit in this study. Equations (10) and (11) are also expressed in matrix and vector form as

$$M\ddot{\boldsymbol{q}} + G\dot{\boldsymbol{q}} = F\boldsymbol{u} \tag{12}$$

where each system matrix has its own elements:

$$M = \begin{bmatrix} I_x & 0 \\ 0 & I_z \end{bmatrix}, \qquad G = \begin{bmatrix} 0 & h_x \\ -h_z & 0 \end{bmatrix}, \qquad F = \begin{bmatrix} 1 & 0 \\ 0 & 1 \end{bmatrix} \tag{13}$$

The mass matrix M is symmetric positive definite, as is the case for most dynamical systems, but G is a skew-symmetric matrix. This is a typical characteristic of gyroscopic systems. Skew-symmetric matrices do not allow modal decomposition, in general, and we work with physical coordinates (ϕ, ψ) directly. As discussed earlier, optimal control solutions experienced significant advantage by dealing with modal coordinates for structural systems. From now on, we discuss the optimal control law design for the roll/yaw dynamic equations of motion.

III. Time-Optimal Control Law

Optimal Control Theory

Before we derive the time-optimal solution for the roll/yaw dynamics, general time-optimal control theory is reviewed.[18] Consider a first-order system as

$$\dot{\boldsymbol{x}} = A\boldsymbol{x} + B\boldsymbol{u}, \qquad \boldsymbol{x}(0),\ \boldsymbol{x}(T_f)\ \text{given} \tag{14}$$

where $x \in R^{n\times 1}$, $A \in R^{n\times n}$, $B \in R^{n\times m}$, and $\boldsymbol{u} = [u_1, u_2, \ldots, u_m]^T$. The control input vector satisfies

$$|u_j| \le N_j, \qquad j = 1, 2, \ldots, m \tag{15}$$

For the given linearized first-order system, the time-optimal control problem is stated as finding a control input vector $\boldsymbol{u}$ that minimizes

$$J = \int_0^{T_f} \mathrm{d}t \tag{16}$$

while the system equation and the boundary conditions of Eq. (14) are satisfied.

The optimal control law is obtained by Pontryagin's minimum principle, for which the Hamiltonian of the system expressed as

$$H = 1 + \boldsymbol{\lambda}^T(A\boldsymbol{x} + B\boldsymbol{u}) \tag{17}$$

is to be minimized. The costate vector $\boldsymbol{\lambda} \in R^{n\times 1}$ is evaluated later by satisfying the optimality condition. The resultant optimal control law becomes[18]

$$u_j = -N_j\,\mathrm{sign}\left[b_j^T\boldsymbol{\lambda}\right] \tag{18}$$

where sign[ ] denotes the signum function and b_j is the jth column of B. The costate vector satisfies

$$\dot{\boldsymbol{\lambda}} = -\frac{\partial H}{\partial \boldsymbol{x}} = -A^T\boldsymbol{\lambda} \tag{19}$$

so that

$$\boldsymbol{\lambda}(t) = e^{-A^T t}\boldsymbol{\lambda}(0) \tag{20}$$

This implies that, once we know the initial condition of the costate vector $[\boldsymbol{\lambda}(0)]$, the desired optimal control law is derived. The optimal control problem becomes a two-point boundary value problem with $x(t_f)$ and $\boldsymbol{\lambda}(0)$ needed at different boundary points.[18] As was discussed in Ref. 14, $\boldsymbol{\lambda}(0)$ can be determined by the switching function condition. If the switching times are determined to be $T_1, T_2, \ldots, T_p$, then the switching function

$$b_j^T \boldsymbol{\lambda}(t) = b_j^T e^{-A^T t}\boldsymbol{\lambda}(0) = S\boldsymbol{\lambda}(0) \tag{21}$$

should vanish at those switching times. This leads us to finding the null space of the matrix

$$\begin{bmatrix} b_j^T e^{-A^T T_1} \\ b_j^T e^{-A^T T_2} \\ \vdots \\ b_j^T e^{-A^T T_p} \end{bmatrix} \tag{22}$$

Thus, depending on the number of switching parameters, the null space solution and/or $\boldsymbol{\lambda}(0)$ could be uniquely determined.[14]

Frequency-Domain Approach

Even if the optimal control theory introduced in the preceding section gives us a solution, most practical solution techniques rely on parameter optimization.[7–16] Instead of solving the two-point boundary value problem directly by using differential equations, the switching times (or parameters) are found so that the cost function is minimized while simultaneously satisfying given boundary conditions.[12–16] This approach has been exploited in a series of previous studies. Singh and Vadali used a parameter optimization technique in their recent study[15] for the time-optimal control problem of a structural model. They introduced a so-called time-delay filter in the formulation of the control torque profile. In this study, we take Singh and Vadali's time-delay-filter approach and apply it to the roll/yaw rest-to-rest maneuver.

For parameter optimization, the number of switching instants should be assumed first. For a dynamic system that consists of a rigid-body mode and n flexible modes, the number of switchings turns out to be at most $2n + 1$ (Ref. 16). This leads us to a conjecture that the maximum number of switchings for each roll/yaw channel is equal to three. This is motivated by a rigid-body mode and a nutational mode in the roll/yaw dynamics.

To discuss the time-optimal control torque profile, first we derive the relationship between the roll/yaw responses and the applied inputs. Taking the Laplace transform of both sides of Eqs. (10) and (11), we arrive at

$$\begin{bmatrix} I_x s^2 & h_x s \\ -h_z s & I_z s^2 \end{bmatrix} \begin{bmatrix} \phi(s) \\ \psi(s) \end{bmatrix} = \begin{bmatrix} I_x s\phi(0) + I_x\dot{\phi}(0) + \psi(0)h_x + u_x \\ I_z s\psi(0) + I_z\dot{\psi}(0) - \phi(0)h_z + u_z \end{bmatrix} \tag{23}$$

or

$$\phi(s) = \frac{1}{s}\phi(0) + \frac{s^2\dot{\phi}(0) - sh_x/I_x\dot{\psi}(0) + s^2u_x/I_x - \nu^2 su_z/h_z}{s^2(s^2+\nu^2)} \tag{24}$$

and also

$$\psi(s) = \frac{1}{s}\psi(0) + \frac{s^2\dot{\psi}(0) + sh_z/I_z\dot{\phi}(0) + \nu^2 su_x/h_x + s^2u_z/I_z}{s^2(s^2+\nu^2)} \tag{25}$$

where $\nu = \sqrt{(h_x h_z/I_x I_z)}$ represents the frequency of the roll/yaw nutational motion. As expected, the roll/yaw angle responses are dynamically coupled by the roll/yaw control inputs as well as the initial nutational motion [$\dot{\phi}(0)$ and $\dot{\psi}(0)$].

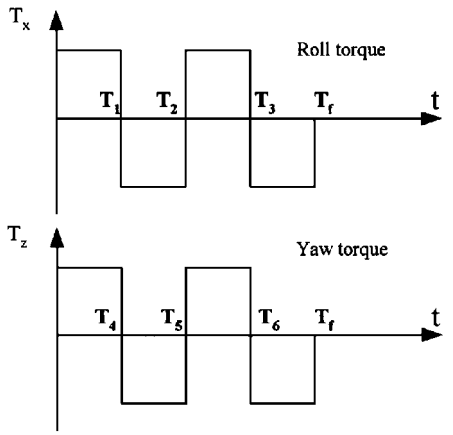

Fig. 2 Minimum-time switching profile for roll/yaw control inputs.

Rest-to-Rest Maneuver

The time-optimal control torque profile is represented by a time-delay filter, as was discussed in Ref. 15. For a rest-to-rest maneuver, the majority of previous approaches took a symmetric control profiles. However, because our application is a gyroscopic system, we temporarily assume a general torque profile with three switching times for each channel, as shown in Fig. 2. The time-delay filter of Fig. 2 can be mathematically modeled as

$$\begin{aligned} u_x(s) &= \frac{M_x}{s(1 - 2e^{-sT_1} + 2e^{-sT_2} - 2e^{-sT_3} + e^{-sT_f})} \\ u_z(s) &= \frac{M_z}{s(1 - 2e^{-sT_4} + 2e^{-sT_5} - 2e^{-sT_6} + e^{-sT_f})} \end{aligned} \tag{26}$$

where M_x and M_z represent the magnitudes of the roll and yaw torques, respectively. The key principle of the time-delay filter was to cancel the rigid and flexible modes by zeros of numerators in Refs. 15 and 16. Without loss of generality, we apply the same principle to control the rigid and nutational modes of the roll/yaw dynamics. First, we show that the time-delay filter cancels the rigid-body mode. The transfer functions in Eq. (26),

$$\begin{aligned} G_x(s) &\equiv 1 - 2e^{-sT_1} + 2e^{-sT_2} - 2e^{-sT_3} + e^{-sT_f} \\ G_z(s) &\equiv 1 - 2e^{-sT_4} + 2e^{-sT_5} - 2e^{-sT_6} + e^{-sT_f} \end{aligned} \tag{27}$$

have at least one zero at $s = 0$ because $G_x(0)$ and $G_z(0) = 0$, respectively. The time-delay filter in Refs. 15 and 16 possesses two zeros at $s = 0$ due to the symmetric torque profile. However, for the nonsymmetric torque profile, only a single zero is guaranteed to exist.

Next, the nutational mode is canceled in the same fashion as flexible mode control, by requiring the transfer functions to vanish at $s = \pm\nu i$. By substituting $s = \pm\nu i$ into Eq. (27) and setting both real and imaginary parts equal to zero, we obtain

$$\begin{aligned} 1 - 2\cos\nu T_1 + 2\cos\nu T_2 - 2\cos\nu T_3 + \cos\nu T_f &= 0 \\ 2\sin\nu T_1 - 2\sin\nu T_2 + 2\sin\nu T_3 - \sin\nu T_f &= 0 \end{aligned} \tag{28}$$

for the roll channel. Note that, when the switching profiles are symmetric with $T_3 = 2T_2 - T_1$, $T_f = 2T_2$, the preceding equations reduce to a single equation as in Refs. 15 and 16. Similarly, for yaw control input,

$$\begin{aligned} 1 - 2\cos\nu T_4 + 2\cos\nu T_5 - 2\cos\nu T_6 + \cos\nu T_f &= 0 \\ 2\sin\nu T_4 - 2\sin\nu T_5 + 2\sin\nu T_6 - \sin\nu T_f &= 0 \end{aligned} \tag{29}$$

To prescribe the relationship between the final roll/yaw pointing angles and control torque inputs, Eq. (26) is substituted into Eqs. (24) and (25). As a consequence,

$$\phi(s) = \frac{sM_xG_x(s)/I_x - \nu^2 M_zG_z(s)/h_z}{s^2(s^2+\nu^2)} \tag{30}$$

and

$$\psi(s) = \frac{\nu^2 M_x G_x(s)/h_x + s M_z G_z(s)/I_z}{s^2(s^2+\nu^2)} \tag{31}$$

These expressions still do not provide explicit information on the final roll/yaw angles and the applied torques. By assuming that the rest-to-rest maneuver condition is always satisfied, we use the final-value theorem of the Laplace transform. The final-value theorem is applicable only in cases where final values exist. In our case, the time-delay filter is designed to cancel the nutational and rigid-body modes exactly. This guarantees that the roll/yaw angles reach constant values over $t \geq T_f$. Application of the final-value theorem yields

$$\phi(T_f) = \lim_{s\to 0} s\phi(s) = -(M_z/h_z)(2T_4 - 2T_5 + 2T_6 - T_f) \tag{32}$$

$$\psi(T_f) = \lim_{s\to 0} s\psi(s) = (M_x/h_x)(2T_1 - 2T_2 + 2T_3 - T_f) \tag{33}$$

Note that the final angles are cross coupled: yaw torque creates roll angle, and vice versa. The final angles can be used as additional constraints to be satisfied by the switching times.

Prior to the application of the optimization algorithm, we discuss the symmetry issue of switching times. In the majority of previous studies, the control input profiles for the rest-to-rest maneuver were set to be symmetric.[12–16] This property has been a great advantage in numerical computation because the number of design parameters to be optimized is reduced by half. Let us assume that the roll/yaw switching profiles are symmetric:

$$\begin{aligned} T_f &= 2T_5, \qquad & T_6 &= 2T_5 - T_4 \\ T_f &= 2T_2, \qquad & T_3 &= 2T_2 - T_1 \end{aligned} \tag{34}$$

The final angles in Eqs. (32) and (33) then become

$$\phi(T_f) = 0, \qquad \psi(T_f) = 0 \tag{35}$$

The final angles become zero with symmetric switching times. The zero final angles constitute significant contrast from nongyroscopic systems, for which symmetric torque inputs result in nonzero final angular displacement. The switching times should be nonsymmetric for nonzero final angular displacements for this specific example of gyroscopic systems.

Because of the nonsymmetric property of switching times, the number of switching parameters is equal to seven: six (T_1, T_2, T_3, T_4, T_5, T_6) from each channel and one for the final time (T_f). However, the optimal solution may be used either in the roll or the yaw channel separately. The optimization problem is restated as finding the seven switching times that minimize

$$J = T_f \tag{36}$$

subject to Eqs. (29) and (30) and to the terminal boundary constraints on roll/yaw angles in Eqs. (32) and (33). To ensure that the solution obtained is a true optimal solution, we augment the constraint equation (21) into the optimization algorithm. The state transition matrix $e^{-A^T t}$ is computed as

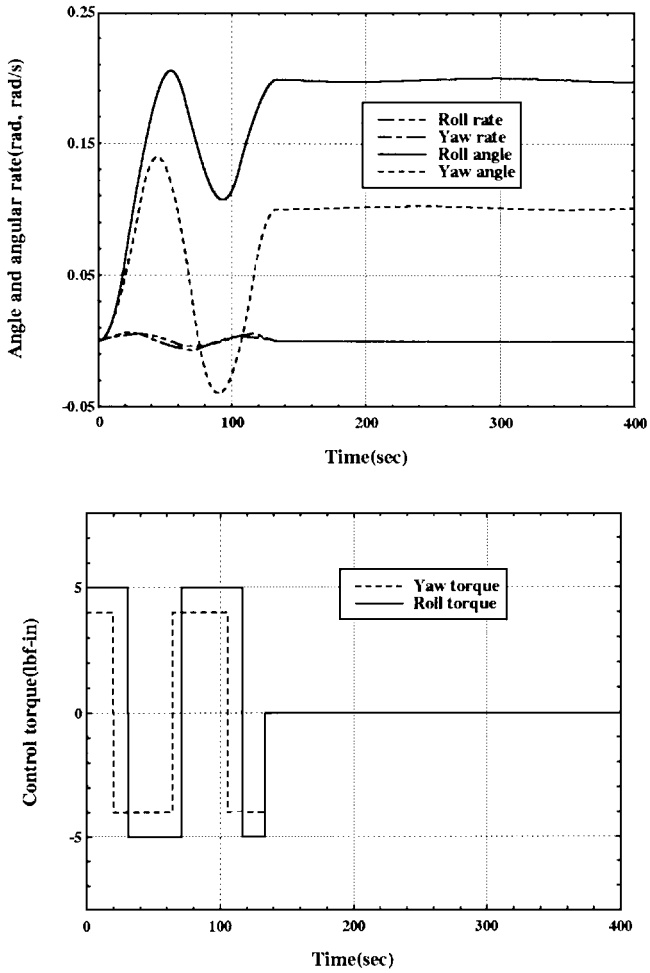

Fig. 3 Simulation results with optimized switching parameters, case 1.

A similar procedure can be used for the yaw channel parameters (T_4, T_5, T_6).

An example spacecraft model used in this study has material property data $I_x = 16{,}572$ in.-lbf-s^2, $I_y = 3552$ in.-lbf-s^2, $I_z = 15{,}468$ in.-lbf-s^2, and $h_w = 475$ in.-lbf-s, which is a geosynchronous communication satellite. Several cases of optimization results using the MatLab Optimization Toolbox[19] are provided in Table 1. The control torques are assumed to be $[M_x, M_z] = [5.0, 4.0]$ lbf-in. for cases 1 and 2 and $[M_x, M_z] = [5.0, -4.0]$ lbf-in. for cases 3 and 4. As discussed earlier, no symmetry exists among the optimized switching times. Simulations using the optimization results are presented in Figs. 3 and 4. The control law is applied to the linearized system only. To fully examine the control law, the same control law needs to be applied to the original nonlinear governing equations of Eqs. (3) and (4). It is easily expected that some pointing error may occur in this case in spite of the small angle and angular rate region used in the simulation.

$$\begin{bmatrix} 1 & 0 & 0 & 0 \\ 0 & 1 & 0 & 0 \\ -(1/\nu)\sin\nu t & (h_z/I_z\nu^2) f(t) & \cos\nu t & -(h_z/I_z\nu)\sin\nu t \\ -(h_x/I_x\nu^2)(1-\cos\nu t) & -(1/\nu)\sin\nu t & (h_x/I_x\nu)\sin\nu t & \cos\nu t \end{bmatrix} \tag{37}$$

where $f(t) \equiv (1 - \cos\nu t)$. Thus, Eq. (21) indicates that the initial costate vector can be found by computing the null space of

$$\begin{bmatrix} -(1/\nu)\sin\nu T_1 & (h_z/I_z\nu^2)(1-\cos\nu T_1) & \cos\nu T_1 & -(h_z/I_z\nu)\sin\nu T_1 \\ -(1/\nu)\sin\nu T_2 & (h_z/I_z\nu^2)(1-\cos\nu T_2) & \cos\nu T_2 & -(h_z/I_z\nu)\sin\nu T_2 \\ -(1/\nu)\sin\nu T_3 & (h_z/I_z\nu^2)(1-\cos\nu T_3) & \cos\nu T_3 & -(h_z/I_z\nu)\sin\nu T_3 \end{bmatrix} \tag{38}$$

Table 1 Optimization results for different final angles

Case	Final values	Optimization results ($[T_1, T_2, T_3, \ldots, T_f]$)
1	$\phi = 0.2$	[30.57, 74.45, 121.7, 20.00,
	$\psi = 0.1$	69.67, 110.9, 146.2]
2	$\phi = 0.1$	[20.00, 67.66, 109.0, 22.33,
	$\psi = -0.2$	68.86, 111.5, 141.7]
3	$\phi = -0.3$	[33.31, 78.97, 128.4, 20.00,
	$\psi = 0.1$	74.45, 114.8, 156.1]
4	$\phi = -0.3$	[22.07, 75.19, 116.9, 20.00,
	$\psi = -0.3$	74.45, 114.8, 1.56.1]

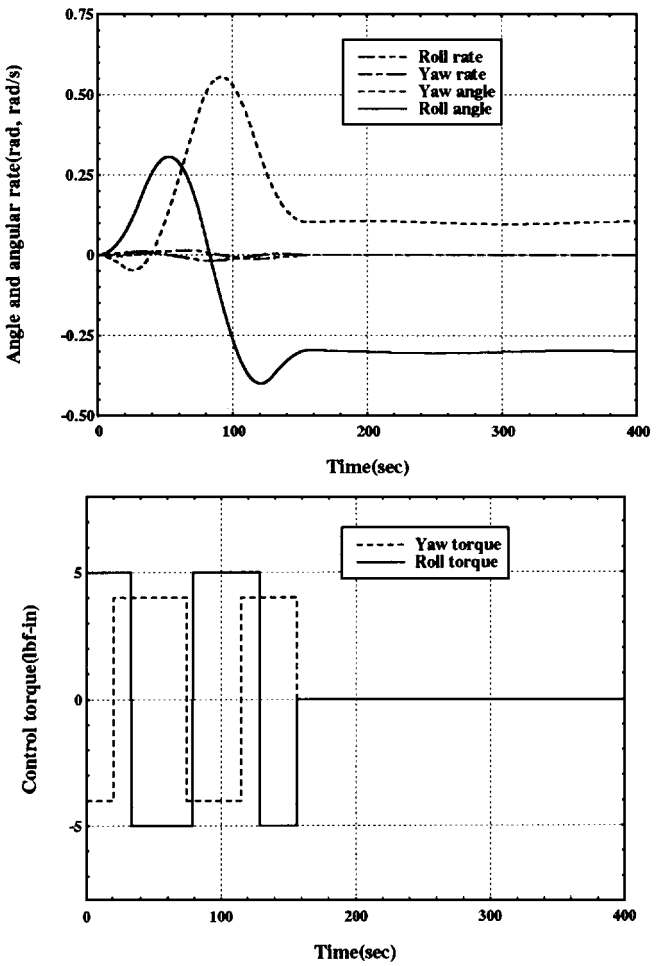

Fig. 4 Simulation results with optimized switching parameters, case 3.

Spin-Up Maneuver

The object of the spin-up maneuver is to maintain constant angular velocity at the final maneuver time. Unlike the rest-to-rest maneuver, therefore, the boundary constraint is placed on the velocity not on the displacement. Let us prescribe the switching profile for the spin-up maneuver in a general form:

$$u_x(s) = (M_x/s)G_x(s), \qquad u_z(s) = (M_z/s)G_z(s) \tag{39}$$

The transfer functions $[G_x(s), G_z(s)]$ in Eq. (39) can be either symmetric or nonsymmetric depending on the boundary condition requirements. As long as $G_x(s)$ and $G_z(s)$ are bang-bang types with terminating control inputs after the maneuver time $[u_x(t) = u_z(t) = 0, t \geq T_f]$, they automatically satisfy

$$G_x(0) = 0, \qquad G_z(0) = 0 \tag{40}$$

That is, there is always at least one zero at $s = 0$, which contributes to cancelling the rigid-body mode. For nutational mode cancellation, the transfer functions must also satisfy

$$G_x(\pm \nu i) = 0, \qquad G_z(\pm \nu i) = 0 \tag{41}$$

To prescribe the spin-up maneuver by the final velocity requirement, first we examine the final velocity expressions. Substitution of Eq. (39) into Eqs. (30) and (31) and application of the final-value theorem yields

$$\dot{\phi}(T_f) = \lim_{s \to 0} s[s\phi(s)] = 0, \qquad \dot{\psi}(T_f) = \lim_{s \to 0} s[s\psi(s)] = 0 \tag{42}$$

Thus, a minimum-time spin-up maneuver with constant final angular velocity is not feasible by a bang-bang control with terminating input after maneuver time. The transfer functions whose numerators cancel the nutational mode produce zero angular velocities at the final maneuver time. This is possible because the gyroscopic mode is coupled with the rigid-body mode. It is also explained by the single pole at $s = 0$ in the original transfer functions of Eqs. (24) and (25), whereas nongyroscopic structural systems have repeated zeros at $s = 0$ (Ref. 15).

IV. Minimum Fuel/Time Control

In this section, the fuel/time-optimal control problem for the roll/yaw dynamics is discussed.[18] First, general fuel/time-optimal control theory is reviewed. The fuel/time-optimal control is stated as finding a control vector $\boldsymbol{u}$ that minimizes

$$J = \int_0^{T_f} (1 + \alpha|\boldsymbol{u}|)\, \mathrm{d}t, \qquad \alpha > 0 \tag{43}$$

subject to the same constraint as Eqs. (14) and (15). In this case, the Hamiltonian of the system becomes

$$H = 1 + \alpha|\boldsymbol{u}| + \boldsymbol{\lambda}^T(A\boldsymbol{x} + B\boldsymbol{u}) \tag{44}$$

The optimal control solution minimizes the Hamiltonian by Pontryagin's principle, so that the resultant control law is given as[16,18]

$$u_j = -\mathrm{dez}\left(b_j^T \boldsymbol{\lambda} / \alpha\right), \qquad j = 1, 2, \ldots, m \tag{45}$$

where u_j is the jth component of $\boldsymbol{u}$ and b_j represents the jth column of B. The costate vector also satisfies

$$\dot{\boldsymbol{\lambda}} = -A^T \boldsymbol{\lambda} \tag{46}$$

and the dead-zone function dez is defined to be[18]

$$a = \mathrm{dez}(b) = \begin{cases} a = 0 & \text{if} \quad |b| < 1 \\ a = \mathrm{sign}(b) & \text{if} \quad |b| > 1 \\ 0 \leq a \leq 1 & \text{if} \quad b = 1 \end{cases} \tag{47}$$

Motivated by Singh's work in Ref. 16 we take the frequency-domain time-delay-filter approach to solve the fuel/time-optimal control problem for the roll/yaw dynamics. Singh solved a benchmark problem of a sample spring-mass model, where the control torque was parameterized as a bang-off-bang configuration with two switches as in Fig. 5. The torque profile in Fig. 5 can be formulated as

$$u_x(s) = (M_x/s)(1 - e^{-T_1 s} - e^{-T_2 s} + e^{-T_f s}) \tag{48}$$

We take a similar approach to the time-optimal case by taking nonsymmetric switching times. The yaw control torque is also parameterized as

$$u_z(s) = (M_z/s)(1 - e^{-T_3 s} - e^{-T_4 s} + e^{-T_f s}) \tag{49}$$

where the switching times (T_3, T_4) match (T_1, T_2) in Eq. (48). The numerators of $u_x(s)$ and $u_z(s)$ automatically possess one zero at

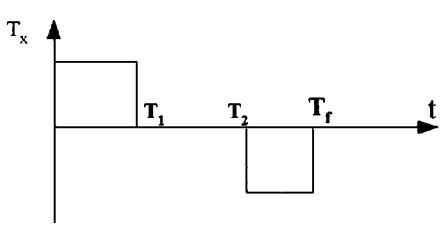

Fig. 5 Bang-off-bang control torque profile.

$s = 0$, regardless of the switching times. The nutational mode is also canceled by requiring

$$1 - \cos(\nu T_1) - \cos(\nu T_2) + \cos(\nu T_f) = 0$$
$$\sin(\nu T_1) + \sin(\nu T_2) - \sin(\nu T_f) = 0 \tag{50}$$

and/or

$$1 - \cos(\nu T_3) - \cos(\nu T_4) + \cos(\nu T_f) = 0$$
$$\sin(\nu T_3) + \sin(\nu T_4) - \sin(\nu T_f) = 0 \tag{51}$$

to be satisfied. Upon the satisfaction of Eqs. (50) and/or (51), it follows that

$$\phi(T_f) = \lim_{s \to 0} s\phi(s) = -(M_z/h_z)(T_3 + T_4 - T_f) \tag{52}$$

$$\psi(T_f) = \lim_{s \to 0} s\psi(s) = (M_x/h_x)(T_1 + T_2 - T_f) \tag{53}$$

Therefore, the optimal fuel/time control problem is reduced to a parameter optimization problem, for which the cost function in Eq. (43) is minimized subject to Eqs. (50–53).

Single Channel Control

Note, however, that the number of parameters is five (T_1, T_2, T_3, T_4, T_f), whereas the total number of constraint equations is six: three for each channel. Thus, a unique solution does not exist for the bang-off-bang formulation of simultaneous roll/yaw control. To have a feasible solution, it is assumed that only one channel is activated. Thus, the number of switching parameters is three: (T_1, T_2, T_f) or (T_3, T_4, T_f). The number of corresponding constraint equations is also three: two for the nutational mode control and one for the final angle constraint.

Let us consider the roll control torque only by setting $u_z(t) = 0$. The cost function is reduced to

$$J = T_f + \alpha M_x(T_1 + T_2 - T_f) \tag{54}$$

There are now three design parameters (T_1, T_2, T_3), and the number of constraint equations is also three: Eqs. (50) and (53). On the other hand, the roll angle is controlled by a yaw torque input by taking $u_z \neq 0$, $u_x = 0$, and T_3, T_4, T_f as switching times.

The optimization algorithm is applied to the cost function of Eq. (54) with a yaw angle constraint. The parameter optimization results can be used to check the optimality condition. By optimality requirement, the following conditions must be satisfied[16]:

$$H(0) = 0, \qquad H(T_f) = 0, \qquad b_1^T \lambda(T_1) = -\alpha, \qquad b_1^T \lambda(T_2) = \alpha \tag{55}$$

which can be rewritten with respect to $\boldsymbol{\lambda}(0)$ as

$$\begin{bmatrix} M_x b_1^T \\ -M_x b_1^T e^{-A^T T_f} \\ b_1^T e^{-A^T T_1} \\ b_1^T e^{-A^T T_2} \end{bmatrix} \begin{bmatrix} \lambda_1(0) \\ \lambda_2(0) \\ \lambda_3(0) \\ \lambda_4(0) \end{bmatrix} = \begin{bmatrix} -1 - \alpha M_x \\ -1 - \alpha M_x \\ -\alpha \\ \alpha \end{bmatrix} \tag{56}$$

where b_1 is the first column of the control input matrix B. It is necessary for the left-hand-side coefficient matrix to be invertible for the switching times obtained by parameter optimization to be a true optimal solution.

The optimization results indicate that different solutions exist depending on initial guessing of parameters (switching times). The final switching times for case 1 are equal to $[T_1, T_2, T_f] = [177.3, 283.6, 319.1]$ s with initial guessing of [100, 200, 300] s. Another case is case 2 for which $[T_1, T_2, T_f] = [390.0, 496.4, 744.5]$ s with initial guessing of [500, 600, 700] s. The final angle constraints for both cases are set to be $[\phi, \psi, \dot{\phi}, \dot{\psi}] = [0, 0.1, 0, 0]$. Simulation results using the optimization result (case 1) are also plotted in Fig. 6.

After trying a number of different initial values, the result of case 1 satisfies

$$T_2 = T_1 + (\pi/\nu), \qquad T_f = 3\pi/\nu \tag{57}$$

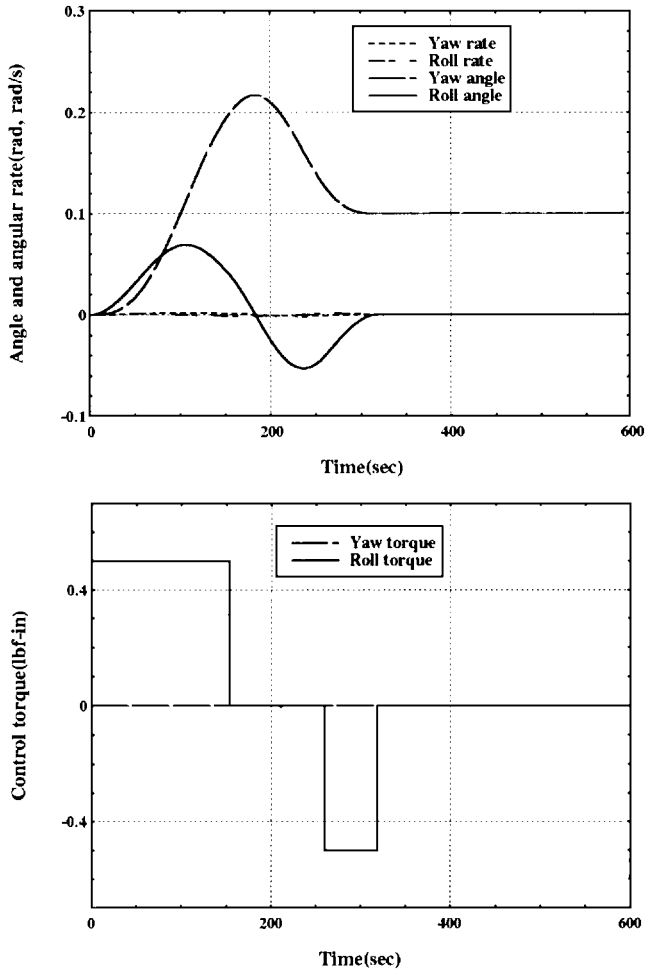

Fig. 6 Simulation result by minimum fuel/time solution, case 1.

and case 2 also satisfies

$$T_2 = T_1 + (\pi/\nu), \qquad T_f = 7\pi\nu \tag{58}$$

There is no guarantee that these solutions are global optimums even though different initial guesses of parameters converge to the identical values. It is easy to show that both cases 1 and 2 satisfy Eqs. (50) and (51), respectively. In addition, note that the final time T_f is fixed regardless of the initial guessing of parameters. By using Eqs. (53) and (57), we can find the ratio between the durations of positive and negative torques in Fig. 5:

$$\frac{T_1}{T_f - T_2} = \frac{-\pi/2\nu + \psi(T_f)h_x/2M_x + T_f/2}{-\pi/2\nu - \psi(T_f)h_x/2M_x + T_f/2} \tag{59}$$

As the final yaw angle $\psi(T_f)$ increases, the ratio increases, too. For maximum yaw angle, it must be satisfied:

$$T_f - T_2 = \frac{-\pi}{2\nu} - \frac{\psi(T_f)_{\max} h_x}{2M_x} + \frac{T_f}{2} = 0 \tag{60}$$

By substituting the final time of case 1, it follows that

$$\frac{-\pi}{2\nu} - \frac{\psi(T_f)_{\max} h_x}{2M_x} + \frac{3\pi}{2\nu} = 0 \tag{61}$$

Therefore,

$$\psi(T_f)_{\max} = (M_x/h_x)(2\pi/\nu) \tag{62}$$

This relationship indicates that the equivalent duration of the applied torque for the maximum yaw angle is equal to one nutational period $2\pi/\nu$.

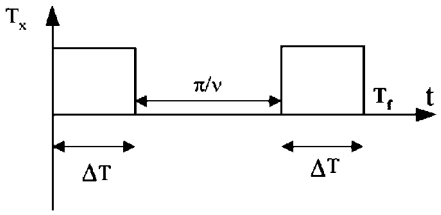

Fig. 7 Single-sided control torque input for nutational motion control.

Single-Sided Firing

For further analysis of the fuel/time-optimal control problem, a well-known principle of gyroscopic systems is introduced. It is familiarly known that gyroscopic systems are controlled by repeated control inputs separated by a certain multiple of the gyroscopic motion frequency. For instance, the roll/yaw nutational motion of a pitch-biased-momentum spacecraft can be controlled by the control torque profile in Fig. 7. The control torque is applied on a single side, which is a significant difference from the earlier case of a double-sided control input of Fig. 5. Moreover, the separation distance between two pulses is equal to the half-nutational period.

The transfer function of the control input profile of Fig. 7 is expressed as

$$u_x(s) = (M_x/s)(1 - e^{-\Delta T})(1 + e^{-\pi s/\nu}) \tag{63}$$

The factor $1 + e^{-\pi s/\nu}$ reflects the pair of identical pulses separated by a half-nutational period. Note that

$$1 + e^{-\pi s/\nu}|_{s=\pm\nu i} = 0 \tag{64}$$

The bang-off-bang control profile, therefore, cancels the nutational mode. The final roll/yaw angular displacements are evaluated as

$$\phi(T_f) = 0, \qquad \psi(T_f) = (M_x/h_x)2\Delta T \tag{65}$$

It is easy to see that the pulse duration time ΔT is directly determined by prescribed $\psi(T_f)$. There is no need for optimization in the control input of Fig. 7. The final maneuver time is determined from

$$T_f = 2\Delta T + \frac{\pi}{\nu} = \frac{h_x \psi(T_f)}{M_x} + \frac{\pi}{\nu} \tag{66}$$

Note that the final maneuver time is proportional to the final yaw angle, which intuitively makes sense. Next, we substitute the maximum yaw angle in Eq. (60) so that

$$T_f = (h_x/M_x)(M_x/h_x)(2\pi/\nu) + (\pi/\nu) = (3\pi/\nu) \tag{67}$$

The final time is equal to that of the optimized results by the double-sided firing. If the final yaw angle is less than $2\pi/\nu$, then the single-sided firing strategy is better than the double-sided firing strategy. This is because the rotational maneuver by single-sided firing takes less time than by the double-sided firing. This also leads us to the conjecture that the two-switch, bang-off-bang control profile may not be the optimal one for this specific application.

V. Conclusions

Optimal time and fuel/time control techniques applied to a pitch bias momentum spacecraft result in control torque profiles that produce optimal rest-to-rest maneuvers. The pitch bias momentum spacecraft linearized equations of motion are decoupled into independent pitch dynamics and gyroscopically coupled roll/yaw dynamics. Both roll and yaw control channels are assumed to switch three times in the time-optimal case. Similarity between a structural flexible mode and a gyroscopic nutational mode was observed and utilized in the control law design. Control switching times for the rest-to-rest maneuver of a gyroscopic system turn out to be nonsymmetric, unlike nongyroscopic structural systems. It also turns out that the minimum-time spin-up maneuver with constant final angular velocity is not possible by a bang-bang torque profile. The minimum fuel/time strategy with two switches may not lead to an optimal solution. Two identical pulses separated by a half-nutational period turns out to be more efficient than the double-sided, two-switch, optimal fuel/time maneuver strategy.

Acknowledgments

The authors would like to acknowledge Korea Telecom for funding this research. Also, the support from Korea Aerospace Research Institute is most valued.

References

[1] Junkins, J. L., and Turner, J. D., *Optimal Spacecraft Rotational Maneuvers*, Elsevier, Amsterdam, 1985, pp. 171–223.

[2] Li, F., and Banium, P. M., "Numerical Approach for Solving Rigid Spacecraft Minimum Time Attitude Maneuvers," *Journal of Guidance, Control, and Dynamics*, Vol. 13, No. 1, 1990, pp. 38–45.

[3] Thompson, R. C., Junkins, J. L., and Vadali, S. R., "Near-Minimum Time Open-Loop Slewing of Flexible Vehicles," *Journal of Guidance, Control, and Dynamics*, Vol. 12, No. 1, 1989, pp. 82–88.

[4] Junkins, J. L., Rahman, Z., and Bang, H., "Near-Minimum-Time Control of Distributed Parameter Systems: Analytical and Experimental Results," *Journal of Guidance, Control, and Dynamics*, Vol. 14, No. 2, 1991, pp. 406–415.

[5] Bilimoria, K. D., and Wie, B., "Minimum Time Larger Angle Reorientation of a Rigid Spacecraft," *Journal of Guidance, Control, and Dynamics*, Vol. 16, No. 3, 1993, pp. 446–452.

[6] Scrivener, S. L., and Thompson, R. C., "Survey of Time-Optimal Attitude Maneuvers," *Journal of Guidance, Control, and Dynamics*, Vol. 17, No. 2, 1994, pp. 225–233.

[7] Meier, E. B., and Bryson, A. E., "An Efficient Algorithm for Time Optimal Control of a Two-Link Manipulator," *Journal of Guidance, Control, and Dynamics*, Vol. 13, No. 5, 1990, pp. 859–866.

[8] Byers, R. M., and Vadali, S. R., "Quasi-Closed Form Solution to the Time-Optimal Rigid Spacecraft Reorientation Problem," *Advances in the Astronautical Sciences*, Vol. 16, No. 4, 1993, pp. 686–694.

[9] Vadali, S. R., Singh, T., and Carter, T., "Computation of Near-Minimum-Time Maneuvers of Flexible Structures by Parameter Optimization," *Journal of Guidance, Control, and Dynamics*, Vol. 17, No. 2, 1994, pp. 354–360.

[10] Singh, G., Kabamba, P. T., and McClamroch, N. H., "Planar Time Optimal, Rest-to-Rest Slewing Maneuvers of Flexible Spacecraft," *Journal of Guidance, Control, and Dynamics*, Vol. 12, No. 1, 1989, pp. 71–81.

[11] Singh, G., Kabamba, P. T., and McClamroch, N. H., "Minimum-Time Maneuvers of Flexible Spacecraft," *Mechanics and Control of Large Flexible Structures*, edited by J. L. Junkins, Vol. 129, Progress in Astronautics and Aeronautics, AIAA, Washington, DC, 1990, pp. 595–637.

[12] Liu, Q., and Wie, B., "Robust Time-Optimal Control of Uncertain Flexible Spacecraft," *Journal of Guidance, Control, and Dynamics*, Vol. 15, No. 3, 1992, pp. 597–604.

[13] Wie, B., Sinha, R., and Liu, Q., "Robust Time-Optimal Control of Uncertain Structural Dynamic Systems," *Journal of Guidance, Control, and Dynamics*, Vol. 16, No. 5, 1993, pp. 980–982.

[14] Ben-Asher, J., Burns, J. A., and Cliff, E. M., "Time-Optimal Slewing of Flexible Spacecraft," *Journal of Guidance, Control, and Dynamics*, Vol. 15, No. 2, 1992, pp. 360–367.

[15] Singh, T., and Vadali, S. R., "Robust Time-Optimal Control: Frequency Domain Approach," *Journal of Guidance, Control, and Dynamics*, Vol. 17, No. 2, 1994, pp. 346–353.

[16] Singh, T., "Fuel/Time Optimal Control of the Benchmark Problem," *Journal of Guidance, Control, and Dynamics*, Vol. 18, No. 6, 1995, pp. 1225–1231.

[17] Agrawal, B. N., *Design of Geosynchronous Spacecraft*, Prentice–Hall, Englewood Cliffs, NJ, 1986, pp. 135–149.

[18] Athans, M., and Falb, P. L., *Optimal Control—An Introduction to the Theory and Its Applications*, McGraw–Hill, New York, 1996, pp. 430–440.

[19] Grace, A., "MatLab, Optimization Toolbox," MathWorks, Inc., Natick, MA, 1994, pp. 3.9–3.12.